Analysis of Multilayered Printed Frequency Selective Surfaces by the MoM/BI-RME Method

Maurizio Bozzi, *Member, IEEE*, and Luca Perregrini, *Member, IEEE*

***Abstract*—This paper presents an efficient method for the analysis of printed periodic structures, consisting of a multilayered array of metal patches in a stratified dielectric medium, illuminated by a uniform plane-wave. These structures are widely used as frequency selective surfaces and mirrors. The analysis is based on the solution of an integral equation by the method of moments (MoM) with entire-domain basis functions. The basis functions are calculated numerically by the boundary integral-resonant mode expansion (BI-RME) method. The patches may have an arbitrary shape, and both metal conductivity and dielectric losses are considered. Some examples are reported to show the accuracy and rapidity of the proposed method.**

***Index Terms*—Coupling integrals, entire domain basis functions, frequency selective surfaces, integral equation.**

I. Introduction

PLANAR arrays of metal patches printed on a dielectric substrate have been widely used as frequency selective surfaces (FSSs) in the microwave and millimeter-wave region [1]–[3]. They find a variety of applications, including quasioptical filters, antenna radomes, subreflectors for multifrequency reflector antennas, and polarizers. The transmission and reflection performance of such structures depends on the shape and size of the metal patches, the periodicity of the array, the thickness and the dielectric characteristics of the substrate. FSSs with patches located on two or more layers and including a stratified dielectric medium (Fig. 1) have been also proposed, with the aim of achieving better performance [1, Ch. 3]. Moreover, printed periodic structures backed by a metal sheet have been used as mirrors [4], [5] and represent the basic elements for the design of reflectarrays [6], [7].

Many methods were adopted for the analysis of FSSs with patches on a dielectric substrate. Among them, the most common technique is based on the formulation of an integral equation, which is solved by the method of moments (MoM) (see, for instance, [1, Ch. 2]). In the application of the MoM, the electric current density on the metal patches is an unknown quantity, which is expressed as a combination of basis functions. The choice of the basis functions is a key-point for the implementation of an efficient algorithm, since a large number of basis functions leads to large matrix problems. In the case of regular shapes (rectangular or circular), entire-domain basis functions can be adopted, which span the entire domain of the patch and satisfy the boundary conditions on its contour [8].

Manuscript received May 31, 2002; revised December 24, 2002.

The authors are with University of Pavia, Department of Electronics, I-27100 Pavia, Italy (e-mail: bozzi@ele.unipv.it; perregrini@ele.unipv.it).

Digital Object Identifier 10.1109/TAP.2003.817996

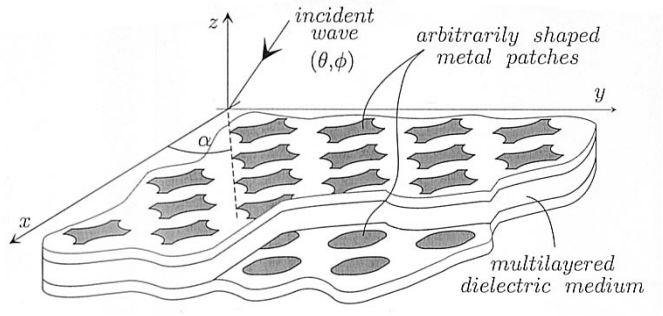

Fig. 1. Frequency selective surface consisting of a periodic array of metal patches with an arbitrary shape. The patches are located on different layers and embedded in a stratified dielectric medium.

These functions are the electric modal vectors of a waveguide with magnetic-wall boundary condition and with a cross-section coincident with the shape of the patch, which correspond to the magnetic modal vectors of a waveguide with electric-wall boundary condition. Whenever possible, the choice of entire-domain basis functions is particularly convenient, since few tens of functions are usually needed for a suitable representation of the unknown current density. Consequently, their use leads to a very efficient implementation of the MoM algorithm. Nevertheless, these functions are available in analytical form only in the case of regular shapes. In a number of particular cases (e.g., cross, tripole, Jerusalem cross) a suitable set of specialized basis functions can be found [9]. In the general case of arbitrary shapes, subdomain basis functions (roof-tops) are typically adopted: they are linear functions defined on a small rectangular or triangular portion of the domain. Such functions are suitable to any kind of patch shape, but usually many hundreds functions are needed [9], and this leads to large MoM matrix problems. This problem becomes even more critical when considering multilayered FSS, since in this case the basis functions are defined on more patches. A partial solution, however, can be found with the method presented in [4], by dividing the structure into many elementary blocks consisting of periodic metallizations between two different dielectric media. The transmission/reflection properties of the FSS are thus obtained by cascading the generalized scattering matrices of each elementary block.

Recently, we proposed a novel algorithm, based on the use of the MoM with entire-domain basis functions defined on arbitrarily shaped domains. In the case of unconventional shapes, the proper set of basis functions is efficiently calculated by the boundary integral-resonant mode expansion (BI-RME) method [10, Ch. 5]. This algorithm is named the MoM/BI-RME method,

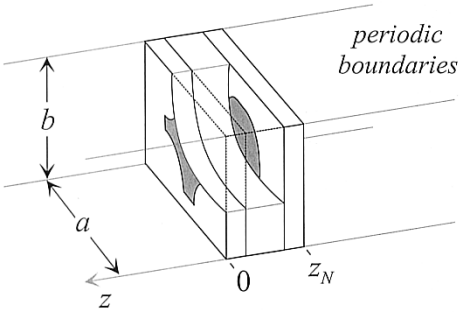

Fig. 2. Elementary cell of the FSS shown in Fig. 1.

and was applied to the analysis of the FSSs consisting of thin [11] or thick perforated metal screens [12], and of boxed microstrip circuits [13].

In this paper, we apply the MoM/BI-RME method to the analysis of printed periodic structures (Fig. 1), consisting of a multilayered array of metal patches in a stratified dielectric medium, possibly grounded by a conductive sheet. The patches may have an arbitrary shape. Losses in both the dielectric medium and the conductors are accounted for.

II. MoM/BI-RME Method

The analysis of printed FSSs is performed under the hypothesis of a multilayered infinite array of metal patches embedded in a stratified dielectric medium. Patches on different layers may have different shapes but must have the same periodicity. The incident field at the frequency ω is a uniform plane wave traveling along an arbitrary direction (θ, ϕ), shown in Fig. 1. Under these hypotheses, the analysis of the whole structure reduces to the investigation of the unit cell with periodic boundary conditions (Fig. 2).

A. Transmission and Reflection Coefficients

An arbitrarily polarized incident plane wave can be expressed as the combination of the two fundamental Floquet modes:

$$\begin{aligned} \vec{\mathcal{E}}'_{00} &= -\nabla\chi_{00}/k_{00} \qquad (\mathrm{TM}_{00}\ \text{mode}) \\ \vec{\mathcal{E}}''_{00} &= -\nabla\chi_{00}\times\vec{u}_z/\mathrm{K}_{00} \qquad (\mathrm{TE}_{00}\ \text{mode}) \end{aligned} \tag{1}$$

in the case of oblique incidence ($\theta \neq 0$), or

$$\begin{aligned} \vec{\mathcal{E}}^0_x &= -\nabla\chi^0_x \quad (\mathrm{TEM}_x\ \text{mode}) \\ \vec{\mathcal{E}}^0_y &= -\nabla\chi^0_y \quad (\mathrm{TEM}_y\ \text{mode}) \end{aligned} \tag{2}$$

in the case of normal incidence ($\theta = 0$). The scalar potentials χ_{rs} are eigenfunctions of the Helmholtz equation with periodic boundary condition, and $k_{rs} = \sqrt{k_{x_{rs}}^2 + k_{y_{rs}}^2}$ are the corresponding eigenvalues, and are given by

$$\chi_{rs} = -\frac{j}{\sqrt{ab}}\, e^{-j(k_{x_{rs}}x + k_{y_{rs}}y)} \tag{3}$$

$$k_{x_{rs}} = k_0 \sin\theta\cos\phi + \frac{2\pi r}{a} \tag{4}$$

$$k_{y_{rs}} = k_0 \sin\theta\sin\phi + \frac{2\pi s}{b} - \frac{2\pi r}{a\tan\alpha} \tag{5}$$

where a and b are the dimensions of the elementary cell (Fig. 2), α is the skew angle (Fig. 1). Moreover, χ^0_x and χ^0_y are eigensolutions of the Laplace equation with periodic boundary condition

$$\chi^0_x = -\frac{x}{\sqrt{ab}} \qquad \chi^0_y = -\frac{y}{\sqrt{ab}}. \tag{6}$$

Therefore, the FSS performance can be easily obtained from matrices $\mathbf{T}$ and $\mathbf{R}$, defined as

$$\begin{bmatrix} \vec{\mathcal{E}}^{\mathrm{I}}_{\mathrm{trans}} \\ \vec{\mathcal{E}}^{\mathrm{II}}_{\mathrm{trans}} \end{bmatrix} = \underbrace{\begin{bmatrix} T^{\mathrm{I\text{-}I}} & T^{\mathrm{I\text{-}II}} \\ T^{\mathrm{II\text{-}I}} & T^{\mathrm{II\text{-}II}} \end{bmatrix}}_{\mathbf{T}} \begin{bmatrix} \vec{\mathcal{E}}^{\mathrm{I}}_{\mathrm{inc}} \\ \vec{\mathcal{E}}^{\mathrm{II}}_{\mathrm{inc}} \end{bmatrix} \tag{7}$$

$$\begin{bmatrix} \vec{\mathcal{E}}^{\mathrm{I}}_{\mathrm{refl}} \\ \vec{\mathcal{E}}^{\mathrm{II}}_{\mathrm{refl}} \end{bmatrix} = \underbrace{\begin{bmatrix} R^{\mathrm{I\text{-}I}} & R^{I\text{-}\mathrm{II}} \\ R^{\mathrm{II\text{-}I}} & R^{\mathrm{II\text{-}II}} \end{bmatrix}}_{\mathbf{R}} \begin{bmatrix} \vec{\mathcal{E}}^{\mathrm{I}}_{\mathrm{inc}} \\ \vec{\mathcal{E}}^{\mathrm{II}}_{\mathrm{inc}} \end{bmatrix} \tag{8}$$

where $\vec{\mathcal{E}}_{\mathrm{inc}}$, $\vec{\mathcal{E}}_{\mathrm{refl}}$, and $\vec{\mathcal{E}}_{\mathrm{trans}}$ are the incident, reflected, and transmitted electric field, respectively, and the superscripts I and II indicate the TM_{00} mode and TE_{00} modes in the case of oblique incidence, and the TEM_x and TEM_y modes in the case of normal incidence.

B. Application of the MoM

A widely used approach for the analysis of printed periodic structures is based on the formulation of an electric field integral equation, which is then solved by the MoM [1, Ch. 2]. This method is briefly described in this section, both for sake of completeness and with the aim of introducing quantities useful for the discussion to follow.

Let us consider a unit cell comprising a total of P metallic patches arbitrarily located at the interfaces of the stratified dielectric medium including N layers (Fig. 2). The analysis is based on the solution of the following $2P$ integral equations

$$\begin{aligned} \vec{\mathcal{E}}^{\mu e}_n(x, y) + \sum_{p=1}^{P} \int_{S_p} \overleftrightarrow{G}(x, y, z_n, x', y', z_p) \cdot \vec{J}^{\mu}_p(x', y')\, dS' \\ = Z_s \vec{J}^{\mu}_n(x, y) \qquad (n = 1, \ldots, P;\ \mu = \mathrm{I}, \mathrm{II}) \end{aligned} \tag{9}$$

obtained by enforcing the boundary condition on the surfaces of all patches. In (9), $\vec{\mathcal{E}}^{\mu e}_n$ is the transverse component of the so-called "excitation field" on the nth patch (i.e., the electric field at the location of the nth patch, in the absence of all patches [4]), Z_s is the "sheet impedance" of the metallizations, S_p indicates the surface of the pth patch, z_p is the longitudinal coordinate of the pth patch, $\vec{J}^{\mu}_p$ is the (unknown) current density on S_p. Finally, $\overleftrightarrow{G}$ is the dyadic Green's function which relates the transverse electric delta current density in (x', y', z_p) to the transverse electric field in (x, y, z_n), given by [14]

$$\overleftrightarrow{G}(x, y, z_n, x', y', z_p) = \sum_m V_m(z_n, z_p) \vec{\mathcal{E}}_m(x, y) \vec{\mathcal{E}}^*_m(x', y') \tag{10}$$

where $\vec{\mathcal{E}}_m$ denotes the transverse electric modal vector of the mth Floquet mode (TE, TM, or TEM), the asterisk denotes the complex conjugate, and functions V_m are determined by considering the equivalent modal transmission lines for the layered

medium in the periodic cell. Note that, for sake of simplicity, a single subscript m is used in the following to indicate the ordered Floquet modes.

Equation (9) is solved by applying the MoM in the Galerkin form. The unknown current density $\vec{J}_p^{\,\mu}$ is represented through a set of N_p basis functions $\vec{e}_{p,\,i}$ defined on the pth patch, namely

$$\vec{J}_p^{\,\mu} = \sum_{i=1}^{N_p} \xi_{p,\,i}^{\mu}\, \vec{e}_{p,\,i} \qquad (p = 1,\, \ldots,\, P) \tag{11}$$

where $\xi_{p,\,i}^{\mu}$ are unknown coefficients.

By substituting (11) in (9) and testing the integral equations by using as test functions $\vec{e}_{p,\,i}$, for each frequency ω we obtain

$$\begin{bmatrix} \mathbf{A}^{1,1} & \cdots & \mathbf{A}^{1,p} & \cdots & \mathbf{A}^{1,P} \\ \vdots & \ddots & & & \vdots \\ \mathbf{A}^{n,1} & \cdots & \mathbf{A}^{n,p} & \cdots & \mathbf{A}^{n,P} \\ \vdots & & \vdots & \ddots & \vdots \\ \mathbf{A}^{P,1} & \cdots & \mathbf{A}^{P,p} & \cdots & \mathbf{A}^{P,P} \end{bmatrix} \begin{bmatrix} \mathbf{X}^{\mathrm{I},1} & \mathbf{X}^{\mathrm{II},1} \\ \vdots & \vdots \\ \mathbf{X}^{\mathrm{I},p} & \mathbf{X}^{\mathrm{II},p} \\ \vdots & \vdots \\ \mathbf{X}^{\mathrm{I},P} & \mathbf{X}^{\mathrm{II},P} \end{bmatrix} = \begin{bmatrix} \mathbf{B}^{\mathrm{I},1} & \mathbf{B}^{\mathrm{II},1} \\ \vdots & \vdots \\ \mathbf{B}^{\mathrm{I},p} & \mathbf{B}^{\mathrm{II},p} \\ \vdots & \vdots \\ \mathbf{B}^{\mathrm{I},P} & \mathbf{B}^{\mathrm{II},P} \end{bmatrix} \tag{12}$$

where

$$\mathbf{A}_{ij}^{n,p} = \sum_m V_m(z_n,\, z_p) \int_{S_n} \vec{e}_{n,j}(x,y) \cdot \vec{\mathcal{E}}_m(x,\, y)\, dS \cdot \int_{S_p} \vec{e}_{p,\,i}(x',\, y') \cdot \vec{\mathcal{E}}_m^{*}(x',\, y')\, dS' + Z_s \delta_{ij} \tag{13}$$

$$\mathbf{B}_i^{\mu,p} = \int_{S_p} \vec{e}_{p,\,i}(x',\, y') \cdot \vec{\mathcal{E}}_p^{\mu e}(x',\, y')\, dS' \tag{14}$$

$$\mathbf{X}_i^{\mu,p} = \xi_{p,\,i}^{\mu} \tag{15}$$

where δ is the Kronecker symbol. Once unknowns $\xi_{p,\,i}$ have been calculated, the transmission and reflection coefficients (7) and (8) can be obtained, following the lines of [8], through the following expressions:

$$T^{\mu\text{-}\nu} = \delta_{\mu\nu} T_d^{\mu\text{-}\nu} + \sum_{p=1}^{P} V^{\mu}(z_N,\, z_p) \sum_{i=1}^{N_p} \xi_{p,\,i}^{\nu} \int_{S_p} \vec{e}_{p,\,i} \cdot \vec{\mathcal{E}}^{\mu *}\, dS \tag{16}$$

$$R^{\mu\text{-}\nu} = \delta_{\mu\nu} R_d^{\mu\text{-}\nu} + \sum_{p=1}^{P} V^{\mu}(0,\, z_p) \sum_{i=1}^{N_p} \xi_{p,\,i}^{\nu} \int_{S_p} \vec{e}_{p,\,i} \cdot \vec{\mathcal{E}}^{\mu *}\, dS \tag{17}$$

where $\mu,\, \nu = \mathrm{I}, \mathrm{II}$, and $T_d^{\mu\text{-}\nu}$ and $R_d^{\mu\text{-}\nu}$ are the transmission and reflection coefficient of the Floquet mode across the multilayered dielectric medium in the absence of the metal patches. Expressions (16) and (17) can be easily extended to the reflection and transmission contribution of the fundamental Floquet mode to higher order modes: in this case, superscript μ refers to the considered upper mode.

C. Entire-Domain Basis Functions

A key feature of the present approach is the use of entire-domain basis functions, i.e., functions which span the entire domain S_p and are tangent to its boundary ∂S_p (like the current density $\vec{J}_p^{\,\mu}$). More specifically, we consider as basis functions the electric modal vectors of a waveguide with a cross-section S_p, bounded by magnetic walls. These modal vectors refers to TM ($\vec{e}'_{p,\,i}$), TE ($\vec{e}''_{p,\,i}$), and, in the case of a multiply connected surface S_p, TEM ($\vec{e}^{\,0}_{p,\,i}$) modes. They can be defined in terms of scalar potentials

$$\vec{e}'_{p,\,i} = -\vec{u}_z \times \frac{\nabla_T \psi'_{p,\,i}}{\kappa'_{p,\,i}} \tag{18}$$

$$\vec{e}''_{p,\,i} = -\frac{\nabla_T \psi''_{p,\,i}}{\kappa''_{p,\,i}} \tag{19}$$

$$\vec{e}^{\,0}_{p,\,i} = -\vec{u}_z \times \nabla_T \psi^0_{p,\,i} \tag{20}$$

where the pairs $\{\psi'_{p,\,i},\, \kappa'_{p,\,i}\}$ and $\{\psi''_{p,\,i},\, \kappa''_{p,\,i}\}$ are the eigensolutions of the homogeneous Helmholtz equation in the domain S_p with Dirichelet and Neumann boundary condition, respectively. In the case of N-times connected surfaces, we have $N-1$ basis functions of the type (20), which are obtained by solving the Laplace equation for $\psi^0_{p,\,i}$ with the boundary condition $\psi^0_{p,\,i} = 1$ on an internal contour and $\psi^0_{p,\,i} = 0$ elsewhere.

When considering arbitrarily shaped patches, the entire-domain basis functions must be determined numerically. The efficiency of the numerical method used for their calculation is of paramount importance, since it practically determines the overall efficiency of the algorithm. For this reason, we use the BI-RME method, which permits the calculation of some tens of eigensolutions of the Helmoltz equation—and, therefore, of basis functions (18) and (19)—in a very short computing time (few seconds on a standard PC). Essentially, the BI-RME method is a modified BI method (BIM), which permits to transform the Helmoltz equation into a linear eigenvalue problem [10, Ch. 5]. The solution of this problem yields, in a single shot, all the eigenvalues $\kappa'_{p,\,i}$ and $\kappa''_{p,\,i}$ up to a prescribed value $\kappa_{\max}$, and the corresponding eigenfunctions $\partial\psi'_{p,\,i}/\partial n_p$ and $\psi''_{p,\,i}$ over the boundary ∂S_p ($\partial/\partial n_p$ is the outward normal derivative on ∂S_p). From these boundary values, potentials $\psi'_{p,\,i}$ and $\psi''_{p,\,i}$ can be calculated on the whole domain S_p, and therefore the basis functions can be obtained through (18) and (19).

In the case of multiply-connected domains, the solution of the Laplace equation by the standard BIM described in [15] provides $\partial\psi^0_{p,\,i}/\partial n_p$ on ∂S_p, and, finally, the basis functions (20).

As an example, Fig. 3 shows some basis functions $\vec{e}'_{p,\,i}$ and $\vec{e}''_{p,\,i}$ in the case of a multiply-connected arbitrary domain, calculated by the BI-RME method.

D. Coupling Integrals

The calculation of the MoM matrices (13) and (14) involves the coupling coefficients

$$\int_{S_p} \vec{e}_{p,\,i}(\vec{r}) \cdot \vec{\mathcal{E}}_m^{*}(\vec{r})\, dS \tag{21}$$

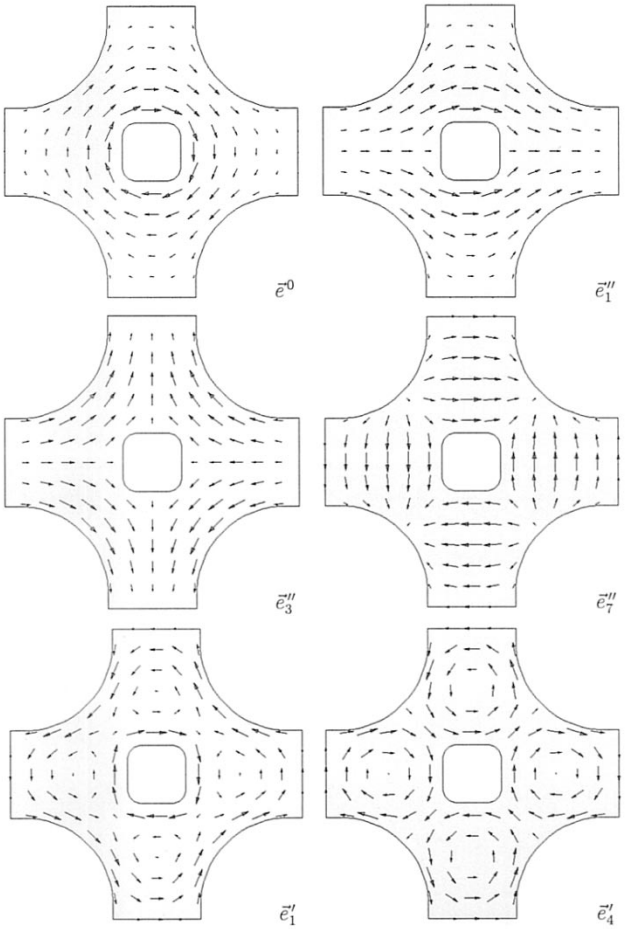

Fig. 3. Some of the first entire-domain vector basis functions used for representing the electric current density on a multiply-connected patch with a rounded cross shape.

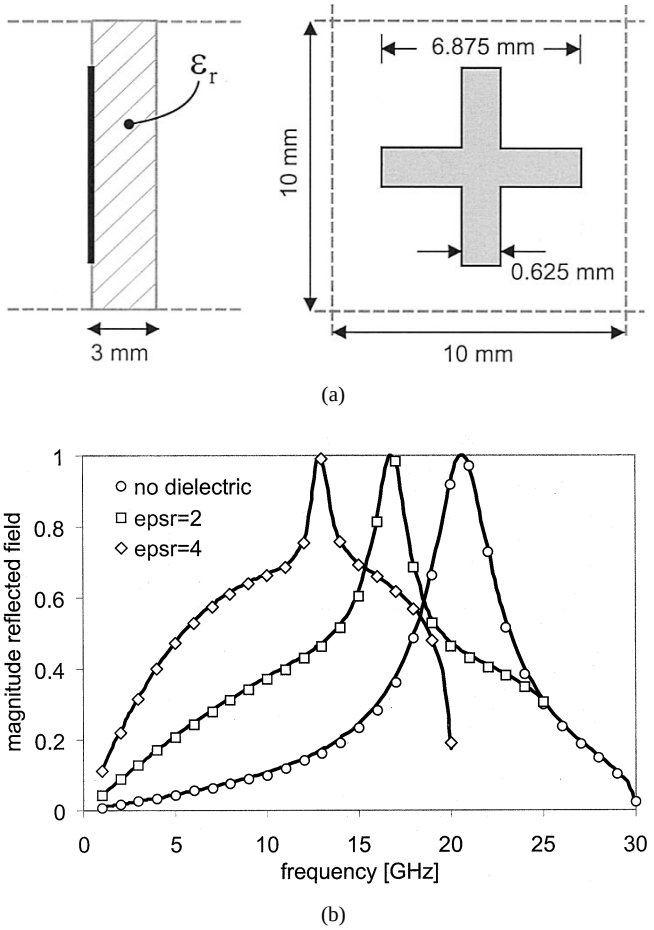

Fig. 4. FSS consisting of cross-shaped patches on a dielectric substrate: (a) side and front view of the unit cell and (b) reflection performance calculated by the MoM/BI-RME method (solid line) compared with simulations reported in the literature (markers).

between the rth basis function on the pth patch and the mth Floquet modal vector. Their evaluation can be directly performed by a surface integration. However, such integration is a time consuming task, especially in cases of basis functions determined by a BI method, since it requires an additional numerical effort for evaluating the basis functions in many points within the integration domain S_p.

By applying the Green's identity and the properties of the modal vectors used as basis functions (see [12, Appendix]), coupling integrals (21) can be transformed from surface to line integrals. In particular, we have

$$\int_{S_p} \vec{e}'_{p,i} \cdot \vec{\mathcal{E}}'^{*}_{m}\, dS = 0 \tag{22}$$

$$\int_{S_p} \vec{e}''_{p,i} \cdot \vec{\mathcal{E}}'^{*}_{m}\, dS = \frac{\kappa''_{p,i}}{k_m(\kappa''^2_{p,i} - k_m^2)} \int_{\partial S_p} \psi''_{p,i}\, \frac{\partial \chi_m^*}{\partial n_p}\, d\ell \tag{23}$$

$$\int_{S_p} \vec{e}^{\,0}_{p,i} \cdot \vec{\mathcal{E}}'^{*}_{m}\, dS = 0 \tag{24}$$

$$\int_{S_p} \vec{e}'_{p,i} \cdot \vec{\mathcal{E}}''^{*}_{m}\, dS = \frac{k_m}{\kappa'_{p,i}(\kappa'^2_{p,i} - k_m^2)} \int_{\partial S_p} \chi_m^*\, \frac{\partial \psi'_{p,i}}{\partial n_p}\, d\ell \tag{25}$$

$$\int_{S_p} \vec{e}''_{p,i} \cdot \vec{\mathcal{E}}''^{*}_{m}\, dS = \frac{1}{\kappa''_{p,i} k_m} \int_{\partial S_p} \psi''_{p,i}\, \frac{\partial \chi_m^*}{\partial t_p}\, d\ell \tag{26}$$

$$\int_{S_p} \vec{e}^{\,0}_{p,i} \cdot \vec{\mathcal{E}}''^{*}_{m}\, dS = -\frac{1}{k_m} \int_{\partial S_p} \chi_m^*\, \frac{\partial \psi'^{0}_{p,i}}{\partial n_p}\, d\ell \tag{27}$$

$$\int_{S_p} \vec{e}'_{p,i} \cdot \vec{\mathcal{E}}^{0}_{m}\, dS = 0 \tag{28}$$

$$\int_{S_p} \vec{e}''_{p,i} \cdot \vec{\mathcal{E}}^{0}_{m}\, dS = \frac{1}{\kappa''_{p,i}} \int_{\partial S_p} \psi''_{p,i}\, \frac{\partial \chi_m^0}{\partial n_p}\, d\ell \tag{29}$$

$$\int_{S_p} \vec{e}^{\,0}_{p,i} \cdot \vec{\mathcal{E}}^{0}_{m}\, dS = 0 \tag{30}$$

where $\partial/\partial t_p$ is the derivative along the boundary, namely in the direction of $\vec{t_p} = \vec{u}_z \times \vec{n}_p$.

The evident advantage of this transformation comes from the possibility of calculating the coupling integrals by a one-dimensional numerical integration. Furthermore, the contour integrals involve $\partial\psi'_{p,i}/\partial n_p$, $\psi''_{p,i}$, and $\partial\psi^0_{p,i}/\partial n_p$ which are obtained as the basic output of the BI-RME analysis. For this reason, the use of the BI-RME method leads to a dramatic computational advantage.

Finally, it is worthy observing that, in cases where $\kappa^2_{p,i} = k_m^2$, expression (23) and (25) are not applicable. Recently, we found a solution to this problem, deriving alternative line-integral expressions, which are applicable also in the cases where

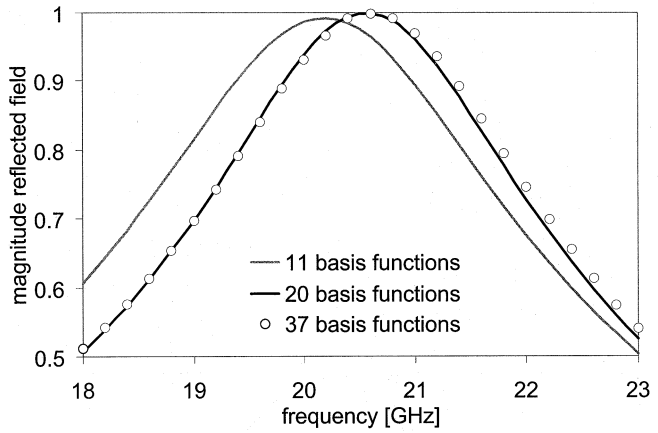

(a)

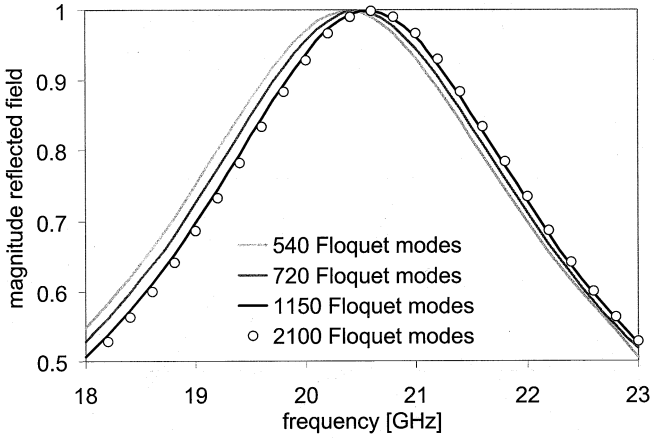

(b)

Fig. 5. Study of the convergence for the free-standing FSS in Fig. 4 when varying the number of basis function (with 1150 Floquet modes) and the number of Floquet modes (with 20 basis functions).

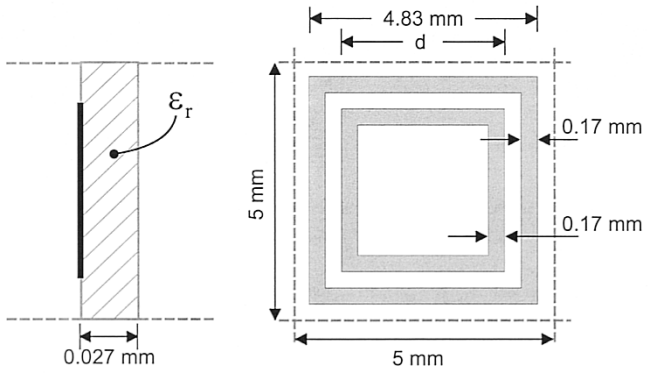

(a)

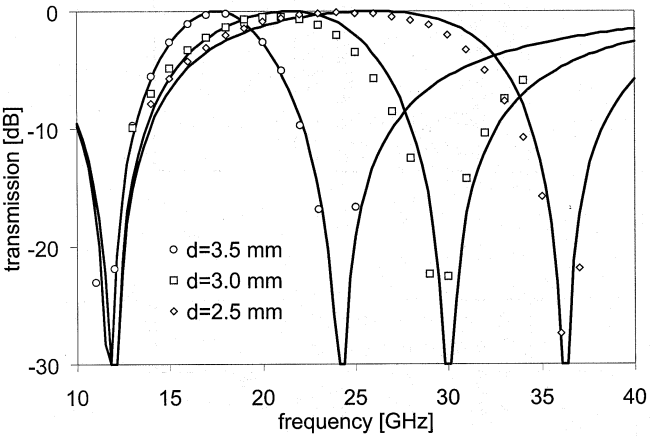

(b)

Fig. 6. FSS comprising two centered square loops on a dielectric substrate: (a) side and front view of the unit cell and (b) transmission performance calculated by the MoM/BI-RME method (solid line) compared with measurements (markers) for different dimensions d of the inner loop (dielectric constant $\varepsilon_r = 3$).

$\kappa''^2_{p,i} = k^2_m$ [16]. By applying this procedure in the case of Floquet modes, we obtain

$$\int_{S_p} \vec{e}''_{p,i} \cdot \vec{\mathcal{E}}'^{*}_{m}\, dS = \frac{\kappa''_{p,i}}{k^2_m(\kappa''_{p,i}+k_m)} \int_{\partial S_p} \psi''_{p,i}\, \frac{\partial \tilde{\chi}^*_m}{\partial n_p}\, d\ell \tag{31}$$

$$\int_{S_p} \vec{e}'_{p,i} \cdot \vec{\mathcal{E}}''^{*}_{m}\, dS = \frac{1}{\kappa'_{p,i}(\kappa'_{p,i}+k_m)} \int_{\partial S_p} \tilde{\chi}^*_m\, \frac{\partial \psi'_{p,i}}{\partial n_p}\, d\ell. \tag{32}$$

Function $\tilde{\chi}_m$ is a modified scalar potential, defined as

$$\tilde{\chi}_m = \frac{\sigma}{\sqrt{ab}}\, e^{-j((\kappa+k_m)/k_m)(\sigma/2)}\, \mathrm{sinc}\left(\frac{\kappa - k_m}{2\pi k_m}\sigma\right) \tag{33}$$

where $\sigma = k_{x_m}x + k_{y_m}y$ and $\mathrm{sinc}(\alpha) = \sin(\pi\alpha)/\pi\alpha$. Moreover $\kappa = \kappa''_{p,i}$ when using in $\tilde{\chi}_m$ in (31), whereas $\kappa = \kappa''_{p,i}$ when using in $\tilde{\chi}_m$ in (32).

When κ and k_m are very different, expressions (31) and (32) still hold true, but their use is less convenient than (23) and (25) from a computational point of view, due to the higher complexity of the integrand function. Thus, the use of (23) and (25) should be preferred.

III. Validation Examples

The MoM/BI-RME method described in the previous Section was implemented in a computer code in Fortran language, running on PC Windows platform. In this Section, some examples are reported, to validate the MoM/BI-RME method and to show the performance of the implemented computer code.

The first example refers to a periodic array of cross-shaped patches in a square grid [17], whose geometry is sketched in Fig. 4(a). The FSS is illuminated by a uniform plane wave incident from the normal direction. Different values of the dielectric constant ε_r of the substrate were considered in the analysis. By using the MoM/BI-RME method, the convergence was achieved with 20 entire-domain basis functions and 1150 Floquet modes. The overall CPU time for the calculation of the frequency response in 100 frequency points was 9 s on a PC Pentium 4 @ 1.7 GHz (6 s for the calculation of the basis functions, and 0.03 s for each frequency point). The MoM/BI-RME results show and excellent agreement with the simulations reported in [17] [Fig. 4(b)]. In the case of the free-standing FSS, a convergence study of the MoM/BI-RME method is also reported. The FSS was analyzed, varying the number of basis functions with a fixed number of Floquet

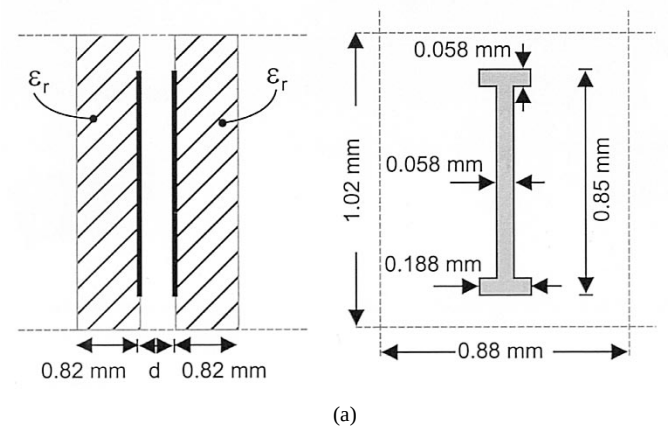

(a)

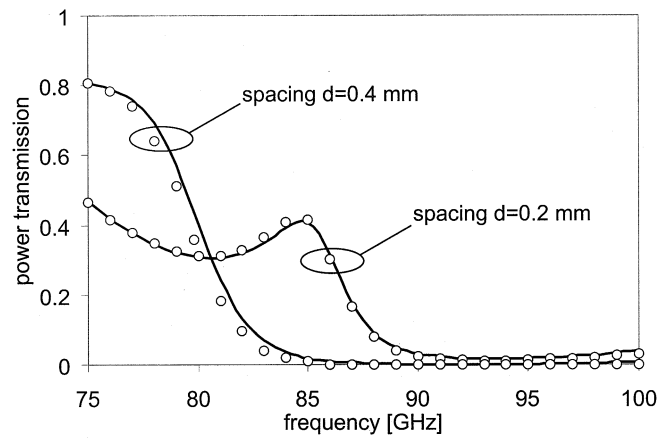

(b)

Fig. 7. Double layer FSS with dogbone-shaped patches with metal losses ($Z_S = 0.3331 + j\,0.008\,88\ \Omega/\square$): (a) side and front view of the unit cell and (b) power transmission of the FSS for different values of the spacing between the layers (dielectric constant $\varepsilon_r = 3.8$).

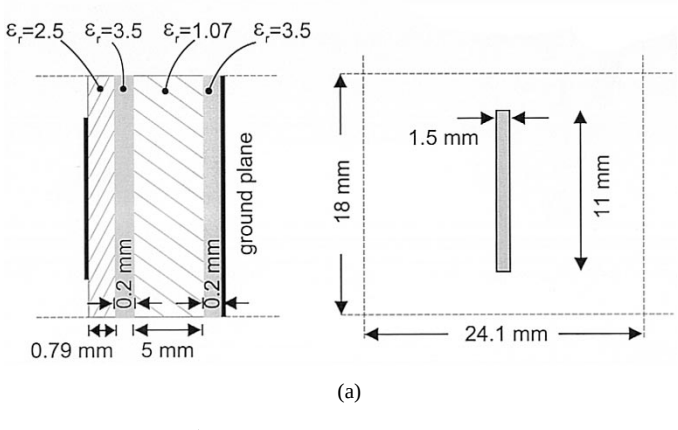

(a)

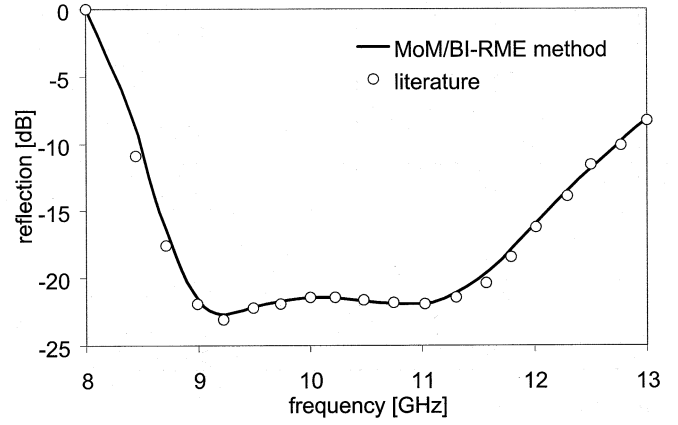

(b)

Fig. 8. Periodic array of rectangular patches on a grounded multilayered dielectric medium: (a) side and front view of the unit cell and (b) reflection coefficient of the fundamental mode versus frequency.

modes [Fig. 5(a)], and varying the number of Floquet modes with a fixed number of basis functions [Fig. 5(b)].

The second example refers to a more complex structure, which comprises two, multiply-connected patches per unit cell. It consists of a square grid of two centered square loops located on a dielectric substrate [Fig. 6(a)] [18]. The incident field is a uniform plane wave incident from the normal direction. Analyzes were performed by considering different dimensions d of the inner loop. The convergence of the analysis by the MoM/BI-RME method was obtained by using 22 basis functions and about 2000 Floquet modes. The symmetry of the metal patches were exploited in the calculation of the basis functions. The overall CPU time for the calculation of the frequency response in 100 frequency points was 15 s on a PC Pentium 4 @ 1.7 GHz. As shown in Fig. 6(b), the simulation results obtained by the MoM/BI-RME method are in very good agreement with measurements reported in [18].

The third example refers to a FSS with metal patches located on two levels [Fig. 7(a)], firstly presented in [19]. The patches have a dogbone shape and present a finite resistivity $Z_S = 0.3331 + j\,0.008\,88\ \Omega/\square$. The FSS is illuminated by a uniform plane wave, vertically polarized and incident from the normal direction. Fig 7(b) reports the power transmission of the structure for two different values of the spacing d between the two layers. The MoM/BI-RME results are compared with simulations reported in [4], where the structure is analyzed by using the MoM with subdomain basis functions, and exhibit a very good agreement. The convergence of the MoM/BI-RME method was obtained with 19 entire-domain basis functions on each metallization and 570 Floquet modes. It is worthy observing that a 28×42 grid discretization was employed in [4], resulting in more than 120 rooftop basis functions. The overall CPU time for the calculation of the frequency response in 100 frequency points was 9 s on a PC Pentium 4 @ 1.7 GHz.

The last example refers to a reflection grating, firstly presented in [20], which suppresses the reflected wave of the fundamental mode, and maximizes the contribution to the first upper mode. It consists of an array of rectangular patches on a stratified dielectric substrate backed with a metal plane [Fig. 8(a)], illuminated by a plane wave with oblique incidence ($\theta = 30°$, $\phi = 0°$). The MoM/BI-RME method can be applied to the analysis of reflection gratings by modifying $V_m(z_n, z_p)$ in the expression of the Green's function (10). The analysis by the MoM/BI-RME method was performed with 17 basis functions and 880 Floquet modes. Fig. 8(b) reports the comparison between the MoM/BI-RME results and the simulation data reported in [4]. The overall CPU time for the calculation of the frequency response in 100 frequency points was 15 s on a PC Pentium 4 @ 1.7 GHz.

IV. Conclusion

This paper presented an efficient method for the analysis of frequency selective surfaces, consisting of an array of arbitrarily shaped metal patches in a multilayered dielectric medium. On the one hand, the efficiency of the method depends on the use of entire-domain basis functions in the MoM for representing the unknown current density on the patches; on the other hand, it is due to the very fast calculation of these functions by the BI-RME method. Moreover, we reported new line-integral expressions for the evaluation of coupling integrals, which are particularly convenient when used in conjunction with the BI-RME method (as well as with any other BI method). A set of examples showed the efficiency of the MoM/BI-RME method in the analysis of different classes of structures, including a periodic array of patches with a ground plane, which represents the basic element in the design of reflectarrays.

References

[1] T. K. Wu, *Frequency Selective Surface and Grid Array*. New York: Wiley, 1995.

[2] J. C. Vardaxoglou, *Frequency Selective Surfaces*. New York: Wiley, 1997.

[3] B. A. Munk, *Frequency Selective Surfaces: Theory and Design*. New York: Wiley Interscience, 2000.

[4] C. Wan and J. A. Encinar, "Efficient computation of generalized scattering matrix for analyzing multilayered periodic structure," *IEEE Trans. Antennas Propagat.*, vol. 43, pp. 1233–1242, Nov. 1995.

[5] C. K. Aanandan, P. Debernardi, R. Orta, R. Tascone, and D. Trinchero, "Problem-matched basis functions for moment method analysis—An application to reflection gratings," *IEEE Trans. Antennas Propagat.*, vol. 48, pp. 35–40, Jan. 2000.

[6] D. M. Pozar, S. D. Targonski, and H. D. Syrigos, "Design of millimeter wave microstrip reflectarrays," *IEEE Trans. Antennas Propagat.*, vol. 45, pp. 287–296, Feb. 1997.

[7] J. A. Encinar, "Design of two–layer printed reflectarrays using patches of variable size," *IEEE Trans. Antennas Propagat.*, vol. 49, pp. 1403–1410, Oct. 2001.

[8] J. P. Montgomery, "Scattering by an infinite periodic array of thin conductors on a dielectric sheet," *IEEE Trans. Antennas Propagat.*, vol. AP-23, pp. 70–75, Jan. 1975.

[9] R. Mittra, C. H. Chan, and T. Cwik, "Techniques for analyzing frequency selective surfaces—A review," *Proc. IEEE*, vol. 76, pp. 1593–1615, Dec. 1988.

[10] G. Conciauro, M. Guglielmi, and R. Sorrentino, *Advanced Modal Analysis*. New York: Wiley, 2000.

[11] M. Bozzi and L. Perregrini, "Efficient analysis of thin conductive screens perforated periodically with arbitrarily shaped apertures," *Electron. Lett.*, vol. 35, no. 13, pp. 1085–1087, June 1999.

[12] M. Bozzi, L. Perregrini, J. Weinzierl, and C. Winnewisser, "Efficient analysis of quasioptical filters by a hybrid MoM/BI-RME method," *IEEE Trans. Antennas Propagat.*, vol. 49, pp. 1054–1064, July 2001.

[13] M. Bozzi, L. Perregrini, A. Alvarez Melcon, M. Guglielmi, and G. Conciauro, "MoM/BI-RME analysis of boxed MMIC's with arbitrarily shaped metallizations," *IEEE Trans. Microwave Theory Tech.*, vol. 49, pp. 2227–2234, Dec. 2001.

[14] L. B. Felsen and N. Marcuvitz, *Radiation and Scattering of Waves*. Englewood Cliffs, NJ: Prentice-Hall, 1973.

[15] G. Conciauro, M. Bressan, and C. Zuffada, "Waveguide modes via an integral equation leading to a linear matrix eigenvalue problem," *IEEE Trans. Microwave Theory Tech.*, vol. MTT-32, pp. 1495–1504, Nov. 1984.

[16] M. Bozzi, G. Conciauro, and L. Perregrini, "On the evaluation of modal coupling coefficients by contour integrals," *IEEE Trans. Microwave Theory Tech.*, vol. 50, pp. 1853–1855, July 2002.

[17] A. S. Barlevy and Y. Rahmat-Samii, "Fundamental constraints on the electrical characteristics of frequency selective surfaces," *Electromagn.*, vol. 17, no. 1, pp. 41–68, Jan.–Feb. 1997.

[18] R. J. Langley and E. A. Parker, "Double square FSS's and their equivalent circuit," *Electron. Lett.*, vol. 19, no. 17, pp. 675–677, Aug. 1983.

[19] T. R. Schimert, A. J. Brouns, C. H. Chan, and R. Mittra, "Investigation of millimeter-wave scattering from frequency selective surfaces," *IEEE Trans. Microwave Theory Tech.*, vol. 39, pp. 315–322, Feb. 1991.

[20] F. S. Johansson, "Frequency-scanned Gratings consisting of photo-etched arrays," *IEEE Trans. Antennas Propagat.*, vol. AP-37, pp. 996–1002, Aug. 1989.

Maurizio Bozzi (S'98–M'01) was born in Voghera, Italy, on June 1, 1971. He received the "Laurea" degree in electronic engineering and the Ph.D. in electronics and computer science from the University of Pavia, Pavia, Italy, in 1996 and 2000, respectively.

From December 1996 to September 1997, he was a Guest Researcher at the Technical University of Darmstadt, Darmstadt, Germany. From October 2001 to January 2002, he was a Postdoctoral Fellow at the University of Valencia, Valencia, Spain. From November to December 2002, he was an Invited Professor at the Polytechnical University of Montreal, Montreal, QC, Canada. Since March 2002, he has been an Assistant Professor of electromagnetics at the Department of Electronics, University of Pavia. His main research activities concern the electromagnetic modeling of frequency selective surfaces, waveguide components, and microwave printed and integrated circuits.

Dr. Bozzi received the Best Young Scientist Paper Award at the XXVII General Assembly of International Union of Radio Science (URSI) in 2002, and the MECSA Prize for the best paper presented by a young researcher at the Italian Conference on Electromagnetics (XIII RINEM) in 2000. He serves on the Editorial Board of the IEEE TRANSACTIONS ON MICROWAVE THEORY AND TECHNIQUES.

Luca Perregrini (M'98) was born in Sondrio, Italy, in 1964. He received the "Laurea" degree in electronic engineering and the Ph.D. in electronics and computer science from the University of Pavia, Pavia, Italy, in 1989 and 1993, respectively.

In 1992, he joined the Department of Electronics, University of Pavia, as an Assistant Professor in electromagnetics where he currently teaches courses in electromagnetic field theory and microwave. He was an Invited Professor at the Polytechnical University of Montreal, Montreal, QC, Canada in 2001 and 2002. He was a Consultant of the European Space Agency and of some European telecommunication companies. His research interests are in numerical methods for the analysis and optimization of waveguide circuits, in the electromagnetic modeling of quasioptical circuits (frequency multipliers, frequency selective surfaces, and reflectarrays) in the millimeter and sub-millimeter wave range, in the modeling of microwave printed and integrated circuits, and in the study of interaction structures for particle accelerators.

Dr. Perregrini serves on the Editorial Board of the IEEE TRANSACTIONS ON MICROWAVE THEORY AND TECHNIQUES, and as a Reviewer for the IEEE TRANSACTIONS ON ANTENNAS AND PROPAGATION.